CHAPTER III

EXPERIMENTAL APPARATUS

To validate the CFD results of the flow phenomena in the R141b ejector and to ensure the optimized model for further CFD simulation, a small experimental ejector refrigeration system was constructed. The system was designed to measure the desired parameters, mainly the performance of an installed ejector in term of its entrainment ratio and the static pressure profile along the wall of the R141b ejector. This section proposes the design and the construction of the experimental refrigerator.

3.1 Refrigerant Selection

It was advised that favorable substance to be selected as a refrigerant flowing through any ejectors should be inflammable, chemically stable, and available. In order to minimize the input energy to the system, its latent heat of evaporation should be as high as possible. The compressibility factor should be nearly the value of 1, so that the ideal gas assumption would be reasonably applied in designing an ejector. Past study [4] showed that the performance of an ejector was increased when molecular weight of the refrigerant was high. Many attempts have been made by using various kind of halocarbon refrigerant such as R11 [5], R12 [6], R113 [7], R123 [8] R134a [9], and R141b [10]. It was found that when using the halocarbon refrigerants, the systems were able to be operated at higher condenser temperatures than that was found in the steam jet refrigerator. The use of R11, R12 and R113 were prohibited and the productions of them are reduced and will finally be eliminated due to their ozone depletion. R123 and R141b are both the replacements of R11 and R113. The ozone depletion potential is 0.02 for R123 and 0.15 for R141b. Even though R141b has a lower molecular weight than that of R123, its boiling point is higher (32°C). The benefit of using the higher boiling point liquid (as high as the room temperature) is that the maintenance and the operation of the system would be easier and cheaper. For example, if the room temperature is below 32°C, when maintenance is needed or there is leakage in the system, there will be only a small chance that R141b will evaporate to the atmosphere and need makeup. This study concentrated only on the use of R141b, since it satisfied the above criteria and was available in the local market at lower cost and higher boiling point than R123. Physical properties of the R141b and R123 are listed in Table 3.1. Although there is a production of R245fa, the new replacement of R11, R123, R141b and R123 and the more environmental friendly, it was not available to the local market at the time of experiment.

Table 3.1 Physical property table for R123 [49] and R141b [50]

Physical properties:	R141b	R123	Unit
Molecular weight	116.95	152.9	
Boiling point under 1.013×10^5 Pa	32.05	27.85	°C
Density of liquid at 25°C	1.227	1.458	g/cm^3
Vapor pressure at 25°C	79	96	kPa
Critical temperature	204.15	183.7	°C
Critical pressure	4.25×10^3	3.67×10^3	kPa
Critical density	0.430	0.549	g/cm^3
Latent heat of vaporization at boiling point	223.0	171.0	kJ/kg
Solubility in water at 25°C	0.509	0.39	% by weight
Specific heat of liquid at 25°C	1.16	0.985	kJ/kg. °C

3.2 Design Concept of the Experimental R141b Ejector Refrigerator

To investigate the flow phenomena and the influences of interested parameters which were thought to affect the performance of an R141b ejector, an experimental ejector refrigeration system was designed as shown in Figure 3.1. The major components of the system were the vapour-generator vessel, the evaporator vessel, the condenser, the receiver tank, the pumping system, and the ejector. The vapour-generator was designed to be able to generate the primary fluid up to 150^{o}C. Two electric immersion heaters were used as simulated heat source and cooling load at the vapour-generator and the evaporator, respectively. The condenser was a plated-heat exchanger type. A liquid refrigerant in the receiver tank was returned back to the vapour-generator and the evaporator via a hydraulic diaphragm pump.

3.3 Construction and Components

Figure 3.1 shows the construction of the experimental R141b ejector refrigerator. All vessels were fabricated from stainless steel 304. Fittings and valves were made from brass. Copper and polyethylene tubes were used as connection lines where the temperature was above and below 50^{o}C, respectively. In the same manner with connection lines, temperature was the criterion of the sealing material selection. Viton A O-rings and Teflon gaskets were used as sealing material of the vapour-generator, where operating temperature exceeds 100^{o}C. For the rest, of which temperature were below 100^{o}C, NBR rubber was selected as the sealing material.

3.3.1 The Vapour-generator

The vessel of the vapour-generator was fabricated from a 6-inch, 120 cm long, schedule 40s, 304 stainless steel pipes with flanges welded at the top and the bottom. A 8 kW immersible electric heater (Figure 3.2) was placed at the lower part of the vessel to generate the primary fluid up to 150^{o}C. Power of the heater was controlled by means of a digital thermostat. At the upper end, three baffles were welded to the vessel to prevent

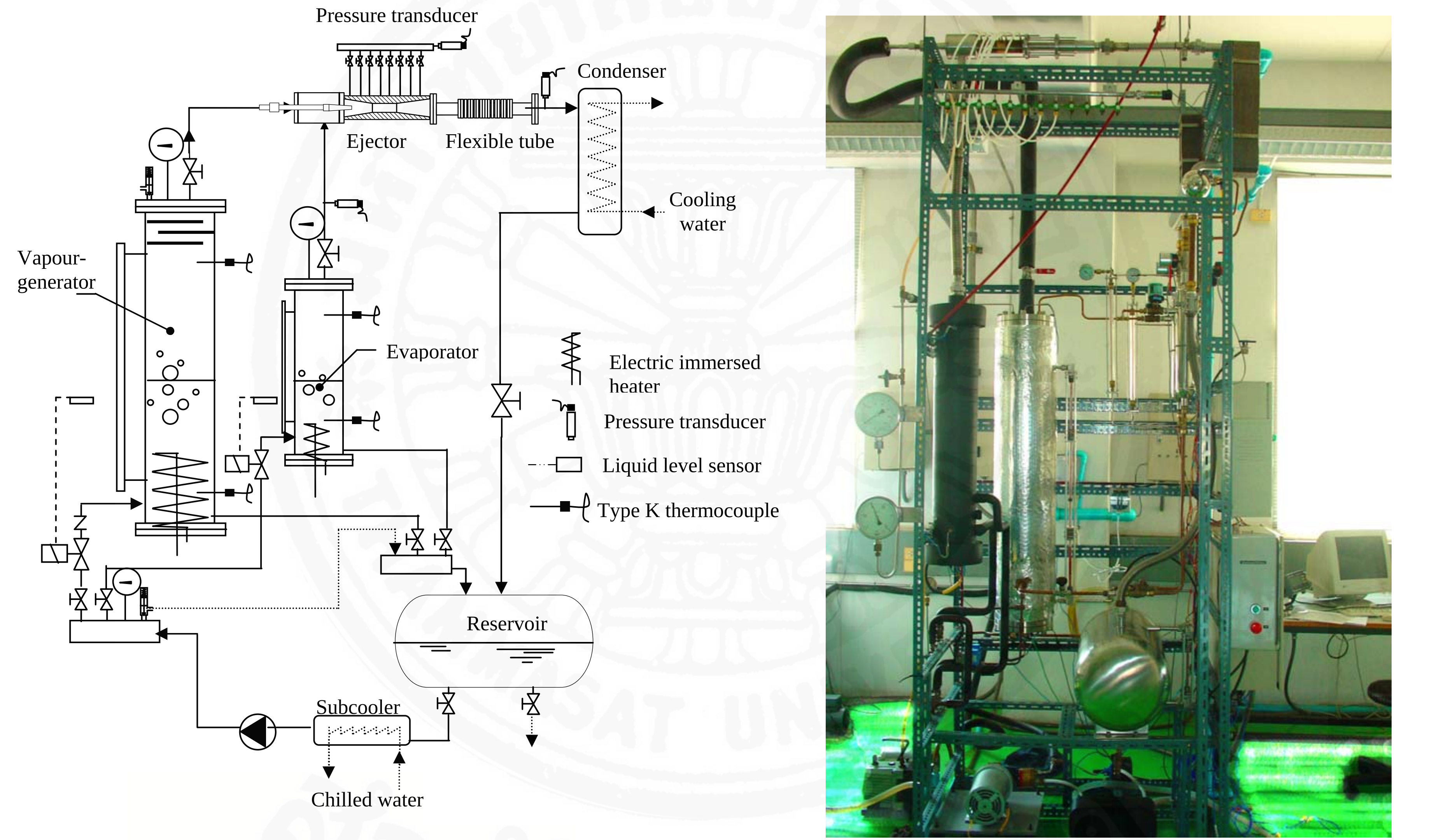

a) b)

Figure 3.1 The experimental R141b ejector refrigerator.

liquid droplets being carried over with refrigerant vapour to the ejector. The vapour-generator was well insulated by a 40 mm thickness of glass fiber wool with aluminum foil backing to prevent the thermal loss from the machine. The level of liquid in the vessel can be observed via the attached sight glass.

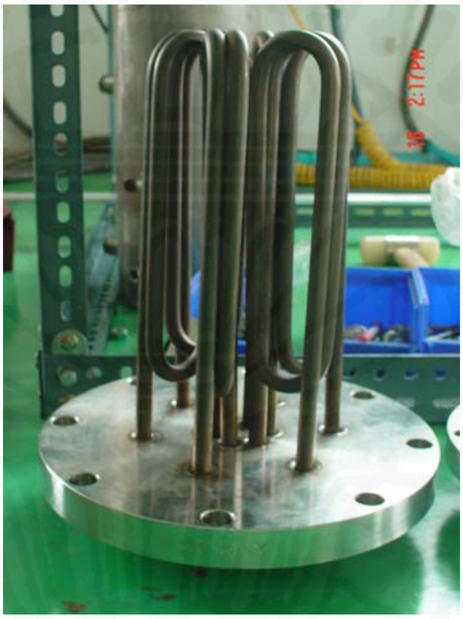

Figure 3.2 The immersible electric heater.

3.3.2 The Evaporator

The evaporator design was similar to the generator. The evaporator shell was fabricated from a 4-inch, 80 cm long, schedule 10s, 304 stainless steel pipe. Similar to that shown in Figure 3.2, a 3 kW immersible electric heater was installed to generate the system cooling load. To prevent the unwanted heat gain from the surrounding, the evaporator was well insulated, by a 30 mm thickness of neoprene foam rubber, from an unexpected heat gain from the environment. The liquid level in the vessel could be observed via the attached sight glass.

3.3.3 The Condenser

A water-cooled plate-type heat exchanger was used as a condenser. The entrance and the exit of the condenser were connected to the other parts of the system using 1-inch, stainless flexible tubes. In addition, an extendable-pipe was connected between the ejector's end and the flexible tube to allow sizing changes of the ejector (Figure 3.3). The liquefied refrigerant was collected in the reservoir tank before it was returned back to the vapour-generator and the evaporator via a pumping system.

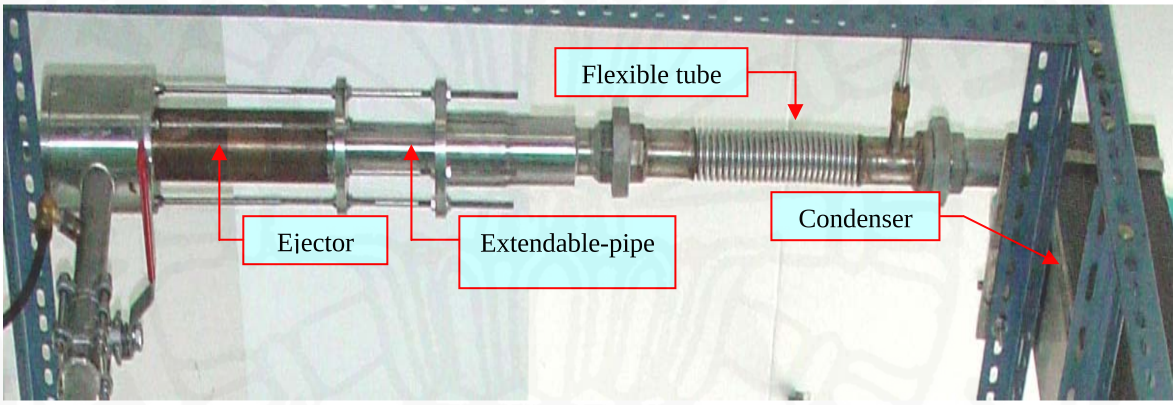

Figure 3.3 Connection of the ejector in the experimental refrigerator.

3.3.4 The Pumping System

Pumping of halocarbon refrigerants such as R11, R123, or R141b is no easy task with commercially available hardware. For example, when R141b is used as the refrigerant, the major difference between R141b and steam-water is their heat of vaporization. At 100°C, for water, the heat of vaporization is around 2,257 kJ/kg compared with 182.8 kJ/kg for R141b. This causes the feeding rate of the vapour-generator for a R141b system to be more than ten times greater than that of the vapour-generator for a steam water system. Due to the large differential pressure across the pump, a positive displacement type pump (gear pump, diaphragm pump, or piston pump) must be used. Both diaphragm pumps and piston pumps are always equipped with a check-valve at the inlet, which will significantly result in pressure drop in the suction-line. Since the liquid refrigerant at the pump inlet is always in saturated condition or slightly sub-cooled, a reduction in pressure, caused by the inlet check-valve, will cause the liquid refrigerant to evaporate and results in cavitations problem. For a gear pump, there is no inlet check valve; therefore, the pressure drop at the inlet is minimal. However, because halocarbon refrigerants, such as R141b, have extremely low lubrication characteristics, this soon will cause the moving parts and mechanical seal to wear away. Therefore, the commercially available pumping system for a jet refrigeration cycle using R141b is more critical than that for a steam-water system.

In this system, a mechanical diaphragm pump (Hydra-Cell Model: F20) as shown in Figure 3.4 was used to circulate liquid refrigerant from the reservoir tank to the vapour-generator and evaporator vessel. This pump was driven by a variable-speed 1 hp electric motor. The hydraulic diaphragm pump is a positive displacement pump which is able to supply maximum flow rate at 4.0 l/min and pressure up to 70 bar. For system protection, a pop-off safety relief valve was installed in the discharge line to bypass the exceed pressure refrigerant back into the receiver tank. Inlet and outlet valves of the pump were stainless steel. The diaphragm and all sealing materials of the pump were selected as Neoprene, the elastomer material resistive to R141b.

As stated previously, in the suction line the refrigerant is always at the saturated phase, so the slightest heat addition or pressure loss causes the cavitations to occur within the pump. This could lead to failure of the valve spring or retainer and diaphragm of the pump. In addition, a subcooler was placed at the inlet line of the diaphragm pump, between the reservoir tank and the pump (Figure 3.4). This subcooler is a small plated heat exchanger which is used to cool the refrigerant down by chilled water obtained from a laboratory's water chiller.

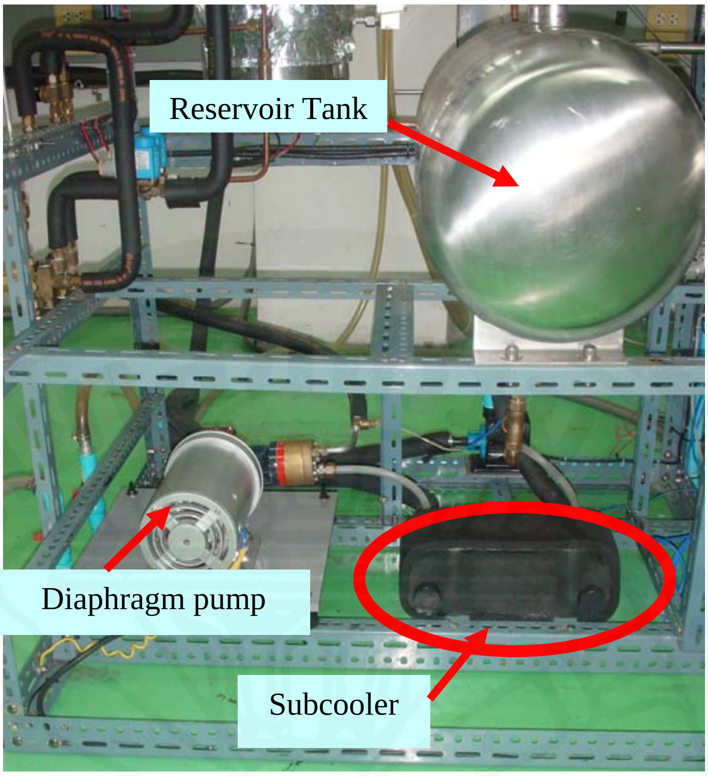

Figure 3.4 The pumping system with the subcooler.

3.4 Instrumentation and Control

In this experimental R141b ejector refrigerator, the operating conditions of each vessel could be controlled separately using the data acquisition system, connected to a personal computer. Parameters to be measured and controlled while the system was operated were temperature, pressure and mass flow rate of the refrigerant.

Type K thermocouples with uncertainties of ± 0.5°C were used to detect the temperature change of the interested position as shown in Figure 3.1. The detected signal of each probe was connected to the compensator and signal amplifier circuit. All probes were carefully calibrated using a precision glass thermometer. Pressures were detected by the absolute pressure transducers. At the evaporator and the pressure manifold, the ranges of the attached transducers were the same at 0-2.0 bar absolute, while the range of the one at the condenser was 0-3.0 bar absolute. All pressure transducers with uncertainties of ±

0.25% were calibrated using a double stage liquid ring vacuum pump and a standard mercury barometer for absolute zero and atmospheric pressure values, respectively.

The operating conditions of the vapour-generator and the evaporator were controlled by applying the ON/OFF logic to the respective heaters. Concerning the condenser, the operating pressure was controlled by adjusting appropriate volume flow rate of cooling water via a flow control valve and an on-off valve in the cooling water circuits. This allowed the system to maintain the operating condition of the condenser at the desired back pressure.

Liquid level in each vessel could be observed by using attached sight glasses. During each test run, the mass flow rates of the refrigerant could be determined by measuring the decreased level of the working fluid, during the certain interval of elapsed time in a steady operation, via the attached sight glasses. This allowed the evaluation of ejector entrainment ratio at the particular operating condition. In addition, for the system to operate continuously, the liquid in the reservoir tank was fed back to the vapour-generator and the evaporator via the pumping system. The liquid level in the evaporator and the vapour-generator were maintained using a variable speed motor drive controller. Electrical power inputs to the heaters (both generator and evaporator) were measured using a digital (Watt-Hour) power analyzer.

3.5 The Ejector

The design of an ejector used in this experiment, the R141b ejector, was based on the one-dimensional analysis of the compressible gas flow through the nozzle and diffuser as described in Appendix A. The following sectional drawing in Figure 3.5 shows the details of the ejector's internal geometry and the connections to other components in the system. The ejector used in the experiment was designed to deliver suction mass of 0.3 kg/min at

0.351 bar abs (5°C saturation temperature) when the primary motive flow rate was 0.96 kg/min at 6.771 bar abs (100°C saturation temperature) and the discharge pressure was 1.33 bar abs. (40°C saturation temperature). The material used for ejector parts was brass. The internal geometry of the ejector was machined employing the EDM technique. A photograph of the ejector used in the experiment is shown in Figure 3.6.

To investigate the flowing and the mixing characteristics at each operating condition, the static pressure was tapped and measured along the vertical axis of the ejector. Polyethylene with 6mm. outer diameter was used as the tapping lines. They were connected to the 8-way pressure manifold and the static pressures were detected by an absolute pressure transducer (0-2.0 bar absolute).

Since geometry of the ejector was one of interested parameters and the recommended dimensions from ESDU [48] were given in the range of numbers, there were 3 primary nozzles, 3 mixing chambers and 3 throats constructed with various sizes. Each of them was designed to be easily fitted and interchanged with others as will be described in the following section. Please note that, the diffuser was thought to have very small influence on ejector performance. Therefore, the studying of effect of the diffuser geometries was omitted and every test was done with only one diffuser.

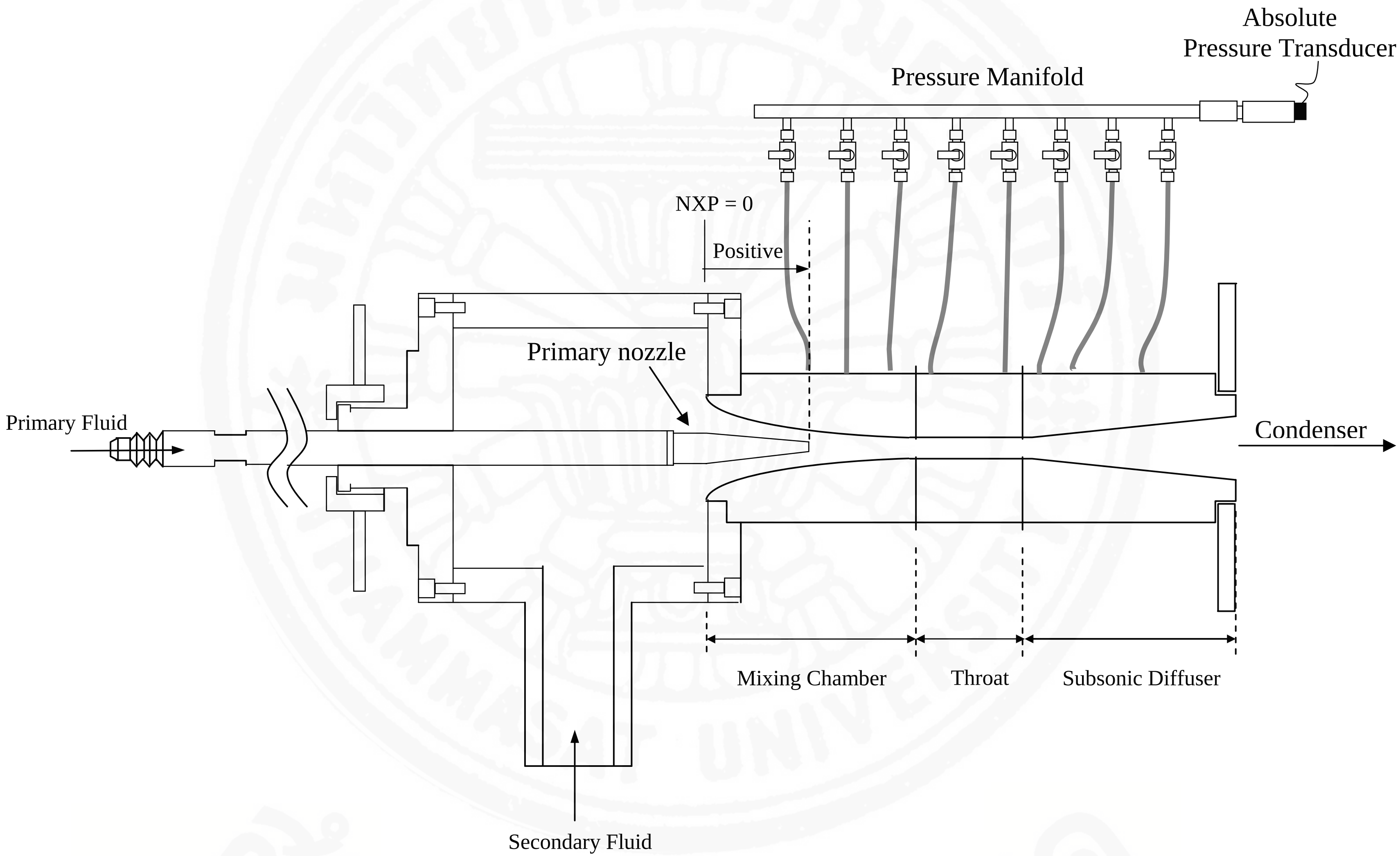

Figure 3.5 Schematic Diagram of Experimental R141b Ejector.

Figure 3.6 Photograph of an ejector used in the expeiment.

3.5.1 The Primary Nozzle

The 3 primary nozzles were constructed with a diameter of 2.5, 2.8 and 3.2 mm at the throat. Nozzle inlets were circular and the exit portions had an included angle of 10°. The ratio of the nozzles throat's diameters to their exit diameter was kept as constant. The nozzle was mounted on the threaded shaft which allowed the axial position of the nozzle in a mixing chamber to be adjusted. The significant geometries of the experiment nozzle are described in Table 3.1. A photograph of the constructed nozzle No.1 is shown in Figure 3.7.

Figure 3.7 Photograph of the primary nozzle.

3.5.2 The Mixing Chamber

There were 3 mixing chambers constructed with 3 different inlet diameters. These allow the investigation of the effect of the mixing chamber's inlet diameters on the ejector performance. Two of them were converging ducts (constant pressure type), while the other one was straight duct (constant area type). For a constant pressure type, the entry sections of the mixing tubes were bell mounted. Other significant dimensions are illustrated in Table 3.2.

3.5.3 The Throat

Four pieces of ejector throat were constructed with the length varying from 2 to 5 times its diameter (8 mm). The cross-sectional area of these throats was constant throughout the conduit. The significant dimensions are described in Table 3.2.

3.5.4 The Subsonic Diffuser

As described previously, only 1 diffuser was constructed. The diffuser has its inlet and exit inside diameters of 8 and 22 mm, respectively. Its cross-sectional area was gradually increased along the length of 77 mm. The detailed dimension of its internal geometry is shown in Table 3.2.

Table 3.2 Ejector's geometry.

Nozzle No.	Primary Nozzle Geometries – D_{th} (mm)	Primary Nozzle Geometries – Y (mm)	Mixing Chamber No.	Mixing Chamber Inlet Diameter – Z (mm)	Throat No.	Throat Length – *l* (mm)	Throat Length – *l* (Times of Diameter)
1	2.8	6.3	1	36	1	16	2d
2	2.5	5.4	2	12	3	32	4d
3	3.2	7.2	3	48	4	40	5d

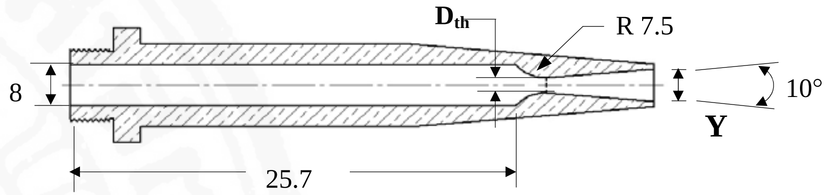

a) Primary nozzle

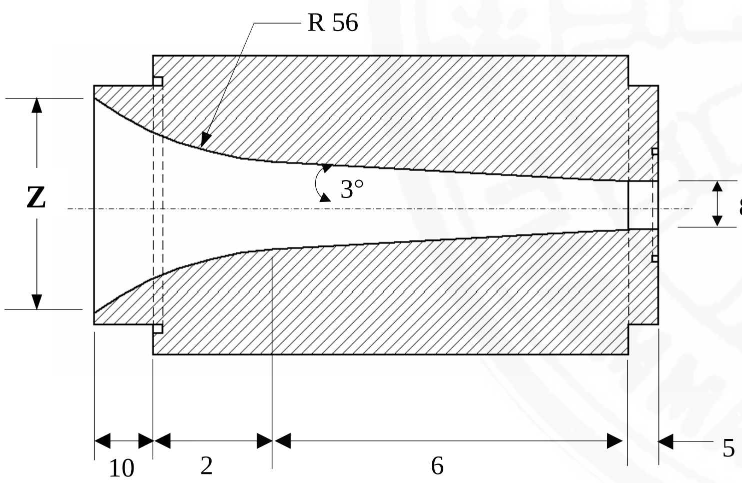

b) Mixing chamber

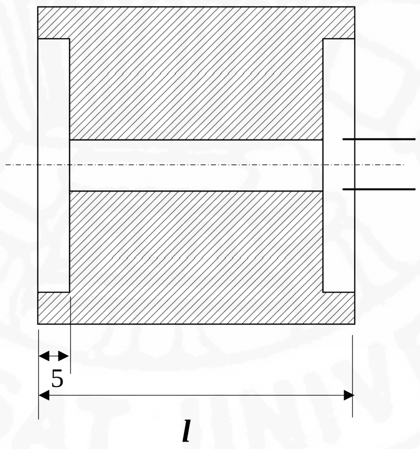

c) Throat

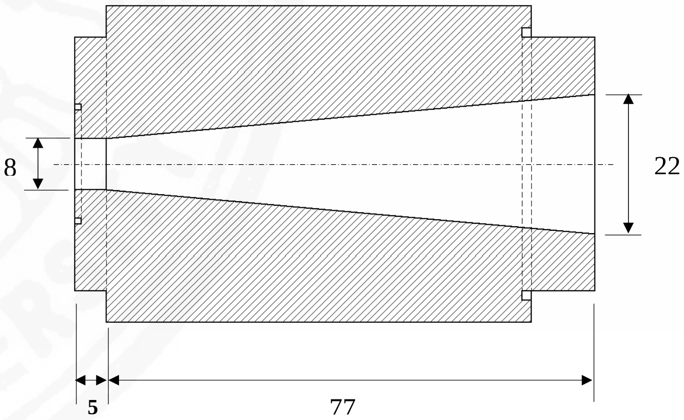

d) Diffuser

3.6 Test Procedures

To start a test, the vapour-generator's heater should be switched on to raise the refrigerant temperature to the desired temperature. The next step was to turn the water pump on. The condenser water valve that was closed could now be opened to allow water to flow through the condenser. After the refrigerant temperature reached its set point on the digital controller key pad, the R141b vapor was released from the top of the vapour-generator to enter the primary nozzle of the ejector by opening the valve at the top of the vapour-generator manually. After the temperature in the vapour-generator was steady, by opening the valve at the top of the evaporator vessel, the secondary flow could be entrained to the ejector and mixed with the primary flow. The refrigerant temperature in the evaporator was also dropped; hence, it was be able to produce a refrigeration effect. To reach the desired evaporator temperature, the evaporator heater was then turned on.

In order to make the system operate continuously, the refrigerant level in the vapour-generator could be maintained by switching on the hydraulic diaphragm pump to feed the refrigerant from the receiver tank via the subcooler back to the vapour-generator and the evaporator. It is recommended that this pump, which is equipped with a speed controller, be set to operate at around 18 Hz at the beginning and then the motor speed could be increased slowly if a higher pressure is required. During the test run, the motor speed and the vapour-generator temperature were responsible for the condition of the primary flow and they could be controlled quite independently without causing too much disruption to the system operation. After the temperature of the refrigerant in the vapour-generator and the evaporator were steady, the primary and secondary mass flow could then be measured as described previously.

3.7 Conclusions

This chapter illustrates the information of the design and construction of the experimental R141b ejector refrigerator. Reasons for choosing R141b as a circulated refrigerant in the system were given. The operating conditions of the constructed test rig were fully automated controlled by a personal computer and data acquisition system. This allows the investigation on the performance characteristics of the ejector. The detailed geometries of the fabricated ejector were described. At the end, the test procedure of the experimental refrigerator was brief. The experimental results based on this experimental refrigerator are provided in Appendix B. The results of the ejector's performance will later be used to validate the CFD results in Chapter V.